Acta Cryst E CRYSTALLOGRAPHIC COMMUNICATIONS

ISSN 2056-9890

N-[2-(Trifluoromethyl)phenyl]maleamic acid: crystal structure and Hirshfeld surface analysis

P. A. Suchetan,[a] Shet M. Prakash,[a] N. K. Lokanath,[b] S. Naveen[c]* and Ismail Warad[d]*

[a]Dept. of Chemistry, University College of Science, Tumkur University, Tumkur, 572 103, India, [b]Department of Studies in Physics, University of Mysore, Manasagangotri, Mysuru 570 006, India, [c]Department of Basic Sciences, School of Engineering and Technology, Jain, University, Bangalore 562 112, India, and [d]Department of Chemistry, Science College, An-Najah National University, PO Box 7, Nablus, Palestinian Territories. *Correspondence e-mail: s.naveen@jainuniversity.ac.in, khalil.i@najah.edu

Received 5 April 2019
Accepted 7 May 2019

Edited by W. T. A. Harrison, University of Aberdeen, Scotland

Keywords: crystal structure; hydrogen bonds; maleamic acids; Hirshfeld surface.

CCDC reference: 1914411

Supporting information: this article has supporting information at journals.iucr.org/e

The title molecule, $C_{11}H_8F_3NO_3$, adopts a *cis* configuration across the –C=C– double bond in the side chain and the dihedral angle between the phenyl ring and side chain is 47.35 (1)°. The –COOH group adopts a *syn* conformation (O=C—O—H = 0°), unlike the *anti* conformation observed in related maleamic acids. In the crystal, inversion dimers linked by pairs of O—H···O hydrogen bonds are connected *via* N—H···O hydrogen bonds and C—H···O interactions into (100) sheets, which are cross-linked by another C—H···O interaction to result in a three-dimensional network. The Hirshfeld surface fingerprint plots show that the highest contribution to surface contacts arises from O···H/H···O contacts (26.5%) followed by H···F/F···H (23.4%) and H···H (17.3%).

1. Chemical context

The development of pH-induced charge-conversion drug-delivery systems can help to overcome the intrinsic pH difference between tumor tissues (pH 6.5–6.8) and normal tissues or the blood stream (pH 7.2–7.4) (Ge *et al.*, 2013). Reactions of 2,3-dimethylmaleic anhydride (DMMA) and amino groups on the particle surface have been used to shield the positive charge of nanoparticles (Du *et al.*, 2010). The generated amide bond is cleavable under mildly acidic conditions but is stable at neutral or basic pH, whereas the DMMA-decorated nanoparticles are inert under physiological conditions. After accumulating into the acidic tumor tissue through the enhanced permeation and retention (EPR) effect, the amide bond slowly cleaves and thus exposes the positive charge, which eventually promotes cell internalization. Therefore, maleamic acids and their derivatives, by virtue of their unique weak acid sensitivity and charge conversion have been widely used as smart carriers to deliver nucleic acids (Meyer *et al.*, 2009), proteins (Zhang *et al.*, 2015; Lee *et al.*, 2007) and drugs (Du *et al.*, 2011; Chen *et al.*, 2015; Han *et al.*, 2015). Simple methods to control the ratio of two positional isomers of mono-substituted maleamic acids and a highly efficient way to synthesize di-substituted maleamic acids have been reported (Su *et al.*, 2017). The hydrolysis profiles of mono- or di-substituted maleamic acids were studied by the same authors to elucidate their hydrolysis selectivity towards various physiologically available pH values (Su *et al.*, 2017). As part our studies in this area, the synthesis and crystal structure of N-[2-(trifluoromethyl)phenyl]maleamic acid, (I),

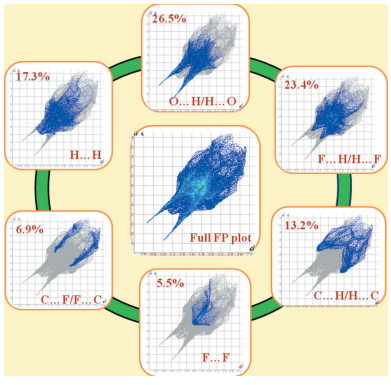

is described and is further analysed using Hirshfeld surfaces and fingerprint plots and compared to related structures.

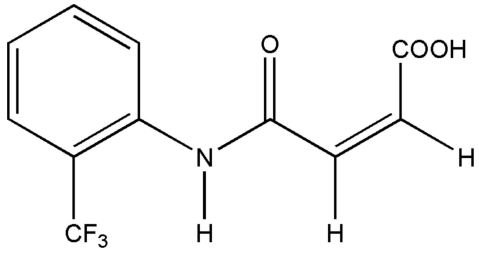

2. Structural commentary

The molecule of (I) adopts a *cis* configuration across the –C═C– double bond in the side chain (Fig. 1), similar to that observed in *N*-(phenyl)maleamic acid (Lo *et al.*, 2009) and other related *o*-substituted maleamic acids, *viz*. *N*-(2-methylphenyl)maleamic acid (Gowda *et al.*, 2010) and *N*-(2-aminophenyl)maleamic acid (Santos-Sánchez *et al.*, 2007). In (I), the dihedral angle between the planes of the phenyl ring C1–C6 and the side chain C1—N1(O1)—C7—C8—C9 is 47.35 (1)° compared to the reported values of 12.7 (1)° in *N*-(2-methylphenyl)maleamic acid (Gowda *et al.*, 2010) and 43.08 (10)° in *N*-(2-aminophenyl)maleamic acid (Santos-Sánchez *et al.*, 2007). Compound (I) differs from related structures in the conformation of its carboxylic acid group. In (I), the –COOH group adopts *syn* conformation (*i.e.* the O3═C10—O2—H2*O* torsion angle = 0°) whereas an *anti* conformation is noted in related structures (the equivalent torsion angle is close to 180°). This disparity is a result of O—H_c···O═C_a (c = carboxylic acid, a = amide) intramolecular hydrogen bonds present in related structures and not observed in (I).

3. Supramolecular features

In the crystal of (I), the molecules are connected *via* pairwise O2—H2*O*···O3 hydrogen bonds (Fig. 2, Table 1) forming $R_2^2(8)$ inversion dimers and N1—H1*N*···O1 hydrogen bonds forming *C*(4) chains (Fig. 2, Table 1), resulting in sheets lying in the (100) plane (Fig. 2). The N1—H1*N*···O1 hydrogen bond is reinforced by a C8—H8···O1 interaction forming another *C*(4) chain in its own right (Fig. 2, Table 1). In addition, C9—H9···O3 interactions (Table 1) forming *C*(4) chains runs down the *b*-axis direction, thereby cross-linking the sheets into a three-dimensional network.

Table 1
Hydrogen-bond geometry (Å, °).

D—H···*A*	*D*—H	H···*A*	*D*···*A*	*D*—H···*A*
N1—H1*N*···O1^{i}	0.86 (2)	2.15 (2)	2.937 (3)	153 (3)
O2—H2*O*···O3^{ii}	0.84 (2)	1.84 (2)	2.679 (3)	179 (7)
C8—H8···O1^{i}	0.93	2.48	3.213 (3)	136
C9—H9···O3^{iii}	0.93	2.49	3.190 (4)	133

Symmetry codes: (i) $x, -y+\frac{3}{2}, z-\frac{1}{2}$; (ii) $-x+1, -y+2, -z+2$; (iii) $-x+1, y+\frac{1}{2}, -z+\frac{3}{2}$.

4. Hirshfeld surface analysis

In the Hirshfeld surface analysis, d_{norm} surfaces and two-dimensional fingerprint plots (FP) were generated to further investigate the intermolecular interactions in (I) and to provide quantitative data for the relative contributions to the surfaces (Turner *et al.*, 2017). The appearance of both dark- and faint-red spots near O1 and O3 support the involvement of each of these atoms in architectures involving the acceptance of a strong hydrogen bond and a weak intermolecular interaction (Fig. 3). Similarly, dark-red spots near the H1*N* and H2*O* hydrogen atoms are due to their involvement as donors in stronger hydrogen bonds, while faint spots near H8 and H9 atoms are due to the weak C—H···O interactions involving these atoms (Fig. 3). Analysis of the fingerprint plots (Fig. 4) showed that the major contributions to the overall Hirshfeld surfaces of (I) are from O···H/H···O (26.5%; $d_i + d_e$ ~1.8 Å), F···H/H···F (23.4%; $d_i + d_e$ ~2.6 Å), H···H (17.3%; $d_i + d_e$

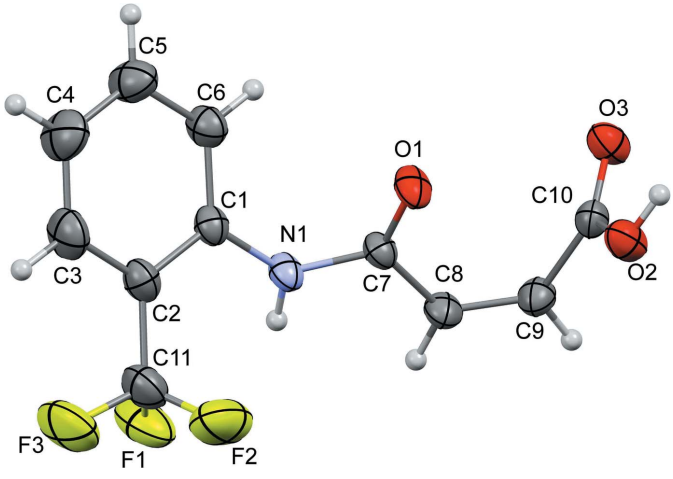

Figure 1
A view of the molecular structure of (I), with displacement ellipsoids drawn at the 50% probability level.

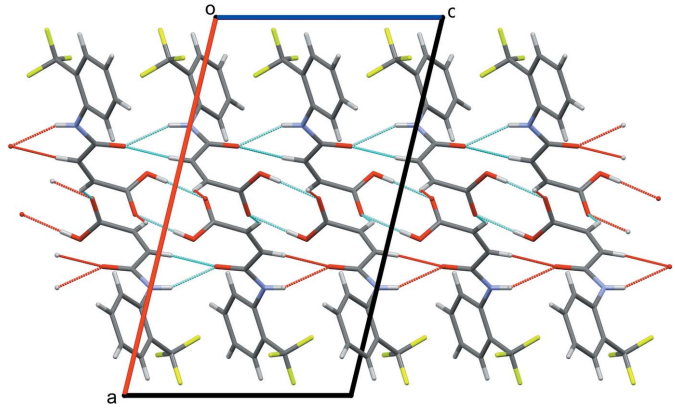

Figure 2
A view down [010] of the crystal packing in (I) showing the sheets of molecules linked by O—H···O and N—H···O hydrogen bonds and C—H···O interactions (thin blue lines).

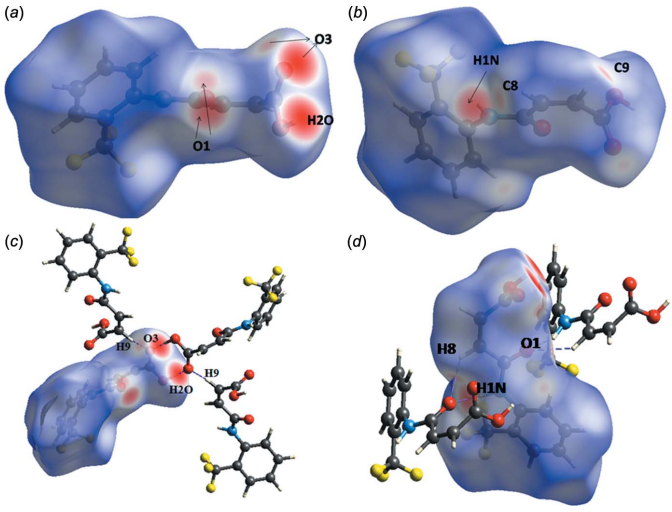

Figure 3
The Hirshfeld surface mapped with d_{norm} for the molecule in (I) over the range −0.753 to 1.252 a.u., shown interacting with near-neighbour molecules connected through hydrogen bonds (dashed lines).

∼2.4 Å), C···H/H···C (13.2%; $d_i + d_e$ ∼3.2 Å), C···F/F···C (6.9%; $d_i + d_e$ ∼3.4 Å) and F···F (5.5%; $d_i + d_e$ ∼3.2 Å) interactions, with other contacts contributing the remaining 10.2%.

5. Database survey

Nineteen *N*-(aryl)-maleamic acids have been reported to date with varied substituents (mono-, di- and trisubstituted derivatives at different positions) on the phenyl ring. Three of these, namely *N*-(phenyl)maleamic acid (CCDC refcode: LOSJUZ) (Lo *et al.*, 2009) and two *o*-substituted compounds, *viz.* *N*-(2-methylphenyl)maleamic acid (QUYJUQ) (Gowda *et al.*, 2010) and *N*-(2-aminophenyl)maleamic acid (PILVAI) (Santos-Sánchez *et al.*, 2007) are closely related to (I), and are therefore of most relevance to the present work. The other 16 structures are either di/tri-substituted compounds or mono-substituted ones at the *meta*/*para* positions. The nature and type of intermolecular interactions, and thereby the resulting architecture in (I) is different from those observed in the three structures, which each feature an *anti* O=C—O—H conformation and an intramolecular O—H···O hydrogen bond, as noted above. In LOSJUZ, adjacent molecules are linked by N—H···O hydrogen bonds into a flat ribbon, while in QUYJUQ, N—H···O hydrogen bonds link the molecules into zigzag chains propagating parallel to [001] and these chains are further linked into sheets by weak π–π interactions. In the crystal structure of PILVAI, symmetry-related molecules are linked by N—H···N hydrogen bonds, forming centrosymmetric amine–amide dimers. The dimers are linked by N—H···O and C—H···O hydrogen bonds and weak N—H···π and π–π interactions into a three-dimensional network.

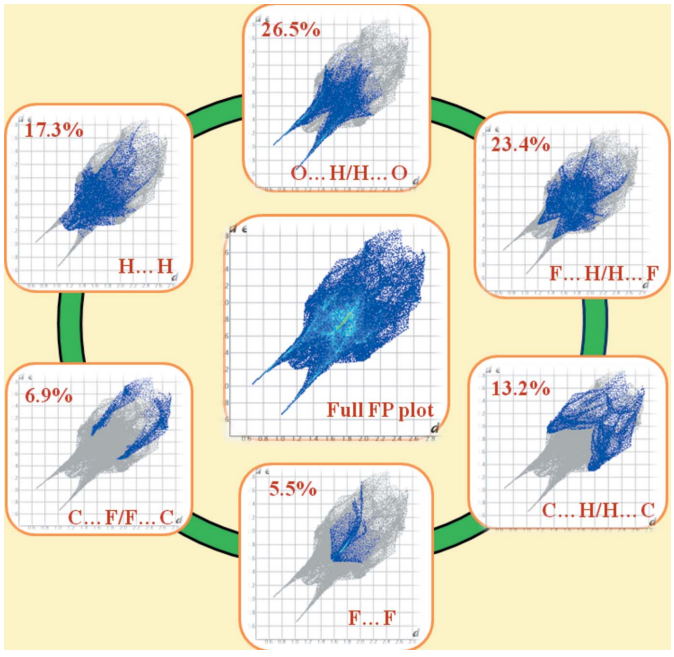

Figure 4
The full two-dimensional fingerprint plot and those delineated into O···H/H···O, F···H/H···F, H···H, C···H/H···C, C···F/F···C and F···F contacts in (I).

Table 2
Experimental details.

Crystal data	
Chemical formula	$C_{11}H_8F_3NO_3$
M_r	259.18
Crystal system, space group	Monoclinic, $P2_1/c$
Temperature (K)	293
a, b, c (Å)	16.307 (4), 7.6438 (16), 9.532 (2)
β (°)	103.669 (8)
V (Å^3)	1154.5 (4)
Z	4
Radiation type	Mo $K\alpha$
μ (mm^{-1})	0.14
Crystal size (mm)	0.22 × 0.19 × 0.17
Data collection	
Diffractometer	Bruker APEXII CCD
Absorption correction	Multi-scan (*SADABS*; Bruker, 2009)
T_{min}, T_{max}	0.970, 0.976
No. of measured, independent and observed [$I > 2\sigma(I)$] reflections	4213, 2598, 1690
R_{int}	0.061
(sin $\theta/\lambda)_{max}$ (Å^{-1})	0.650
Refinement	
$R[F^2 > 2\sigma(F^2)]$, $wR(F^2)$, S	0.065, 0.186, 1.03
No. of reflections	2598
No. of parameters	171
No. of restraints	2
H-atom treatment	H atoms treated by a mixture of independent and constrained refinement
$\Delta\rho_{max}$, $\Delta\rho_{min}$ (e Å^{-3})	0.34, −0.26

Computer programs: *APEX2* and *SAINT-Plus* (Bruker, 2009), *SHELXT2016* (Sheldrick, 2015*a*), *SHELXL2016* (Sheldrick, 2015*b*) and *Mercury* (Macrae *et al.*, 2008).

6. Synthesis and crystallization

The title compound was synthesized by following the same procedure that was employed for synthesizing *N*-(2-methyl-

phenyl)maleamic acid (Gowda *et al.*, 2010). Colourless prisms of (I) were recrystallized from ethanol solution.

7. Refinement

Crystal data, data collection and structure refinement details are summarized in Table 2. The carbon-bound H atoms were placed in calculated positions (C—H = 0.93 Å) and were included in the refinement in the riding-model approximation, with U_{iso}(H) set to 1.2U_{eq}(C). The oxygen- and nitrogen-bound H atoms were located from difference-Fourier maps and freely refined.

Acknowledgements

The authors thank the Institution of Excellence, Vijnana Bhavana, University of Mysore, Manasagangotri, Mysore, for collecting the X-ray diffraction data.

References

Bruker (2009). *APEX2*, *SADABS* and *SAINT-Plus*. Bruker AXS Inc., Madison, Wisconsin, USA.
Chen, J. J., Ding, J. X., Zhang, Y., Xiao, C. S., Zhuang, X. L. & Chen, X. S. (2015). *Polym. Chem.* **6**, 397–405.
Du, J. Z., Du, X. J., Mao, C. Q. & Wang, J. (2011). *J. Am. Chem. Soc.* **133**, 17560–17563.
Du, J.-Z., Sun, T.-M., Song, W.-J., Wu, J. & Wang, J. (2010). *Angew. Chem.* **122**, 3703–3708.
Ge, Z. & Liu, S. (2013). *Chem. Soc. Rev.* **42**, 7289–7325.
Gowda, B. T., Tokarčík, M., Shakuntala, K., Kožíšek, J. & Fuess, H. (2010). *Acta Cryst.* E**66**, o1554.
Han, S. S., Li, Z. Y., Zhu, J. Y., Han, K., Zeng, Z. Y., Hong, W., Li, W. X., Jia, H. Z., Liu, Y., Zhuo, R. X. & Zhang, X. Z. (2015). *Small*, **11**, 2543–2554.
Lee, Y., Fukushima, S., Bae, Y., Hiki, S., Ishii, T. & Kataoka, K. (2007). *J. Am. Chem. Soc.* **129**, 5362–5363.
Lo, K. M. & Ng, S. W. (2009). *Acta Cryst.* E**65**, o1101.
Macrae, C. F., Bruno, I. J., Chisholm, J. A., Edgington, P. R., McCabe, P., Pidcock, E., Rodriguez-Monge, L., Taylor, R., van de Streek, J. & Wood, P. A. (2008). *J. Appl. Cryst.* **41**, 466–470.
Meyer, M., Dohmen, C., Philipp, A., Kiener, D., Maiwald, G., Scheu, C., Ogris, M. & Wagner, E. (2009). *Mol. Pharm.* **6**, 752–762.
Santos-Sánchez, N. F., Salas-Coronado, R., Peña-Hueso, A. & Flores-Parra, A. (2007). *Acta Cryst.* E**63**, o4156.
Sheldrick, G. M. (2015*a*). *Acta Cryst.* A**71**, 3–8.
Sheldrick, G. M. (2015*b*). *Acta Cryst.* C**71**, 3–8.
Su, S., Du, F.-S. & Li, Z.-C. (2017). *Org. Biomol. Chem.* **15**, 8384–8392.
Turner, M. J., Mckinnon, J. J., Wolff, S. K., Grimwood, D. J., Spackman, P. R., Jayatilaka, D. & Spackman, M. A. (2017). *CrystalExplorer17*. University of Western Australia.
Zhang, X., Zhang, K. & Haag, R. (2015). *Biomater. Sci.* **3**, 1487–1496.

supporting information

Acta Cryst. (2019). E**75**, 766-769 [https://doi.org/10.1107/S2056989019006509]

N-[2-(Trifluoromethyl)phenyl]maleamic acid: crystal structure and Hirshfeld surface analysis

P. A. Suchetan, Shet M. Prakash, N. K. Lokanath, S. Naveen and Ismail Warad

Computing details

Data collection: *APEX2* (Bruker, 2009); cell refinement: *SAINT-Plus* (Bruker, 2009); data reduction: *SAINT-Plus* (Bruker, 2009); program(s) used to solve structure: SHELXT2016 (Sheldrick, 2015a); program(s) used to refine structure: *SHELXL2016* (Sheldrick, 2015b); molecular graphics: *Mercury* (Macrae *et al.*, 2008); software used to prepare material for publication: *SHELXL2016* (Sheldrick, 2015b).

N-[2-(Trifluoromethyl)phenyl]maleamic acid

Crystal data

$C_{11}H_8F_3NO_3$
M_r = 259.18
Monoclinic, $P2_1/c$
Hall symbol: -P 2ybc
a = 16.307 (4) Å
b = 7.6438 (16) Å
c = 9.532 (2) Å
β = 103.669 (8)°
V = 1154.5 (4) Å^3
Z = 4
F(000) = 528

Prism
D_x = 1.491 Mg m^{-3}
Melting point: 440 K
Mo $K\alpha$ radiation, λ = 0.71073 Å
Cell parameters from 143 reflections
θ = 3.5–27.5°
μ = 0.14 mm^{-1}
T = 293 K
Prism, colourless
0.22 × 0.19 × 0.17 mm

Data collection

Bruker APEXII CCD diffractometer
Radiation source: fine-focus sealed tube
Graphite monochromator
ω scans
Absorption correction: multi-scan (SADABS; Bruker, 2009)
T_{min} = 0.970, T_{max} = 0.976

4213 measured reflections
2598 independent reflections
1690 reflections with $I > 2\sigma(I)$
R_{int} = 0.061
θ_{max} = 27.5°, θ_{min} = 3.5°
h = −21→12
k = −9→9
l = −12→11

Refinement

Refinement on F^2
Least-squares matrix: full
$R[F^2 > 2\sigma(F^2)]$ = 0.065
$wR(F^2)$ = 0.186
S = 1.02
2598 reflections
171 parameters

2 restraints
Primary atom site location: dual
Hydrogen site location: mixed
H atoms treated by a mixture of independent and constrained refinement
$w = 1/[\sigma^2(F_o^2) + (0.0701P)^2 + 0.4963P]$ where $P = (F_o^2 + 2F_c^2)/3$

$(\Delta/\sigma)_{max} < 0.001$
$\Delta\rho_{max} = 0.34$ e Å^{-3}
$\Delta\rho_{min} = -0.26$ e Å^{-3}

Special details

Geometry. All esds (except the esd in the dihedral angle between two l.s. planes) are estimated using the full covariance matrix. The cell esds are taken into account individually in the estimation of esds in distances, angles and torsion angles; correlations between esds in cell parameters are only used when they are defined by crystal symmetry. An approximate (isotropic) treatment of cell esds is used for estimating esds involving l.s. planes.

Fractional atomic coordinates and isotropic or equivalent isotropic displacement parameters (Å²)

	x	*y*	*z*	U_{iso}*/U_{eq}
O1	0.34076 (13)	0.7544 (3)	0.73122 (17)	0.0570 (5)
O2	0.41280 (13)	1.1030 (3)	0.8624 (2)	0.0604 (6)
O3	0.52092 (13)	0.9298 (3)	0.8536 (2)	0.0609 (5)
N1	0.28493 (13)	0.6788 (3)	0.4975 (2)	0.0475 (5)
F2	0.15299 (15)	0.6837 (4)	0.2366 (2)	0.1062 (8)
F3	0.03339 (14)	0.6184 (4)	0.2675 (3)	0.1295 (11)
C1	0.23369 (16)	0.5362 (3)	0.5229 (2)	0.0457 (6)
F1	0.1069 (2)	0.8137 (3)	0.3972 (3)	0.1357 (12)
C7	0.33398 (15)	0.7774 (3)	0.6013 (2)	0.0425 (6)
C10	0.45863 (17)	1.0115 (3)	0.7934 (3)	0.0465 (6)
C9	0.43322 (18)	1.0235 (4)	0.6336 (3)	0.0523 (7)
H9	0.457140	1.113209	0.590732	0.063*
C8	0.38002 (17)	0.9193 (3)	0.5470 (3)	0.0502 (6)
H8	0.371000	0.935384	0.447771	0.060*
C6	0.26681 (18)	0.4086 (4)	0.6223 (3)	0.0580 (7)
H6	0.322621	0.416324	0.674408	0.070*
C2	0.15006 (17)	0.5244 (4)	0.4447 (3)	0.0546 (7)
C3	0.1014 (2)	0.3826 (5)	0.4683 (4)	0.0756 (9)
H3	0.045544	0.373178	0.416789	0.091*
C5	0.2173 (2)	0.2686 (5)	0.6450 (4)	0.0761 (10)
H5	0.239695	0.183177	0.712740	0.091*
C11	0.1111 (2)	0.6602 (5)	0.3390 (4)	0.0750 (9)
C4	0.1357 (2)	0.2570 (5)	0.5674 (4)	0.0861 (11)
H4	0.102772	0.162430	0.581975	0.103*
H1N	0.285 (2)	0.717 (4)	0.413 (2)	0.072 (10)*
H2O	0.433 (3)	1.094 (6)	0.952 (2)	0.104 (14)*

Atomic displacement parameters (Å²)

	U^{11}	U^{22}	U^{33}	U^{12}	U^{13}	U^{23}
O1	0.0721 (13)	0.0702 (12)	0.0297 (8)	−0.0182 (10)	0.0138 (8)	−0.0043 (8)
O2	0.0620 (12)	0.0664 (13)	0.0500 (11)	0.0158 (10)	0.0073 (9)	−0.0087 (10)
O3	0.0565 (12)	0.0719 (13)	0.0507 (10)	0.0130 (10)	0.0051 (9)	−0.0098 (9)
N1	0.0513 (12)	0.0585 (13)	0.0319 (10)	−0.0109 (10)	0.0085 (8)	−0.0007 (10)
F2	0.0939 (16)	0.152 (2)	0.0649 (12)	−0.0081 (15)	0.0031 (11)	0.0347 (13)
F3	0.0652 (14)	0.161 (2)	0.136 (2)	−0.0054 (16)	−0.0303 (13)	0.0407 (19)
C1	0.0465 (14)	0.0539 (14)	0.0380 (11)	−0.0066 (12)	0.0127 (10)	−0.0059 (11)

F1	0.188 (3)	0.0863 (17)	0.1125 (19)	0.0550 (19)	−0.0055 (18)	0.0035 (15)
C7	0.0436 (13)	0.0517 (13)	0.0319 (11)	−0.0027 (11)	0.0084 (9)	−0.0030 (10)
C10	0.0488 (14)	0.0410 (12)	0.0483 (13)	−0.0048 (11)	0.0089 (11)	−0.0058 (11)
C9	0.0653 (17)	0.0480 (15)	0.0452 (13)	−0.0079 (13)	0.0163 (12)	0.0014 (11)
C8	0.0610 (16)	0.0553 (15)	0.0339 (11)	−0.0063 (13)	0.0104 (11)	0.0031 (11)
C6	0.0467 (15)	0.0666 (18)	0.0597 (16)	−0.0050 (14)	0.0104 (12)	0.0043 (14)
C2	0.0421 (14)	0.0652 (17)	0.0542 (15)	−0.0019 (13)	0.0071 (11)	−0.0063 (14)
C3	0.0479 (16)	0.088 (2)	0.086 (2)	−0.0175 (17)	0.0066 (15)	−0.003 (2)
C5	0.066 (2)	0.071 (2)	0.091 (2)	−0.0053 (17)	0.0175 (17)	0.0224 (19)
C11	0.0561 (19)	0.093 (3)	0.0674 (19)	−0.0018 (19)	−0.0028 (15)	0.005 (2)
C4	0.067 (2)	0.079 (2)	0.112 (3)	−0.0220 (19)	0.020 (2)	0.014 (2)

Geometric parameters (Å, º)

O1—C7	1.230 (3)	C10—C9	1.483 (4)
O2—C10	1.309 (3)	C9—C8	1.316 (4)
O2—H2O	0.845 (18)	C9—H9	0.9300
O3—C10	1.215 (3)	C8—H8	0.9300
N1—C7	1.346 (3)	C6—C5	1.388 (4)
N1—C1	1.428 (3)	C6—H6	0.9300
N1—H1N	0.861 (18)	C2—C3	1.393 (4)
F2—C11	1.328 (4)	C2—C11	1.481 (4)
F3—C11	1.329 (4)	C3—C4	1.369 (5)
C1—C6	1.378 (4)	C3—H3	0.9300
C1—C2	1.394 (4)	C5—C4	1.365 (5)
F1—C11	1.307 (4)	C5—H5	0.9300
C7—C8	1.481 (3)	C4—H4	0.9300
C10—O2—H2O	110 (3)	C1—C6—H6	119.8
C7—N1—C1	124.9 (2)	C5—C6—H6	119.8
C7—N1—H1N	112 (2)	C1—C2—C3	119.1 (3)
C1—N1—H1N	123 (2)	C1—C2—C11	121.8 (3)
C6—C1—C2	119.8 (2)	C3—C2—C11	119.1 (3)
C6—C1—N1	120.4 (2)	C4—C3—C2	120.1 (3)
C2—C1—N1	119.8 (2)	C4—C3—H3	119.9
O1—C7—N1	123.8 (2)	C2—C3—H3	119.9
O1—C7—C8	121.6 (2)	C4—C5—C6	119.6 (3)
N1—C7—C8	114.6 (2)	C4—C5—H5	120.2
O3—C10—O2	123.4 (2)	C6—C5—H5	120.2
O3—C10—C9	121.1 (2)	F1—C11—F3	107.1 (3)
O2—C10—C9	115.4 (2)	F1—C11—F2	106.2 (4)
C8—C9—C10	126.1 (2)	F3—C11—F2	104.4 (3)
C8—C9—H9	116.9	F1—C11—C2	113.4 (3)
C10—C9—H9	116.9	F3—C11—C2	112.6 (3)
C9—C8—C7	122.5 (2)	F2—C11—C2	112.5 (3)
C9—C8—H8	118.7	C3—C4—C5	121.0 (3)
C7—C8—H8	118.7	C3—C4—H4	119.5
C1—C6—C5	120.4 (3)	C5—C4—H4	119.5

C7—N1—C1—C6	−48.6 (4)	C6—C1—C2—C11	178.7 (3)
C7—N1—C1—C2	132.6 (3)	N1—C1—C2—C11	−2.5 (4)
C1—N1—C7—O1	0.7 (4)	C1—C2—C3—C4	0.0 (5)
C1—N1—C7—C8	−179.1 (2)	C11—C2—C3—C4	−178.9 (3)
O3—C10—C9—C8	92.9 (4)	C1—C6—C5—C4	0.6 (5)
O2—C10—C9—C8	−91.3 (4)	C1—C2—C11—F1	−63.2 (4)
C10—C9—C8—C7	3.4 (5)	C3—C2—C11—F1	115.7 (4)
O1—C7—C8—C9	3.0 (4)	C1—C2—C11—F3	175.0 (3)
N1—C7—C8—C9	−177.3 (3)	C3—C2—C11—F3	−6.1 (5)
C2—C1—C6—C5	−0.1 (4)	C1—C2—C11—F2	57.3 (4)
N1—C1—C6—C5	−178.9 (3)	C3—C2—C11—F2	−123.8 (3)
C6—C1—C2—C3	−0.2 (4)	C2—C3—C4—C5	0.4 (6)
N1—C1—C2—C3	178.6 (3)	C6—C5—C4—C3	−0.7 (6)

Hydrogen-bond geometry (Å, º)

D—H···*A*	*D*—H	H···*A*	*D*···*A*	*D*—H···*A*
N1—H1*N*···O1^{i}	0.86 (2)	2.15 (2)	2.937 (3)	153 (3)
O2—H2*O*···O3^{ii}	0.84 (2)	1.84 (2)	2.679 (3)	179 (7)
C8—H8···O1^{i}	0.93	2.48	3.213 (3)	136
C9—H9···O3^{iii}	0.93	2.49	3.190 (4)	133

Symmetry codes: (i) *x*, −*y*+3/2, *z*−1/2; (ii) −*x*+1, −*y*+2, −*z*+2; (iii) −*x*+1, *y*+1/2, −*z*+3/2.